Probing the dynamics of photoexcited carriers in Si₂Te₃ nanowires

Jiyang Chen,¹ Keyue Wu,^{2,3} Xiao Shen,¹ Thang Ba Hoang^{1,*} and Jingbiao Cui¹

¹Department of Physics and Materials Science, The University of Memphis, Memphis, TN 38152, USA

²College of Electrical and Photoelectronic Engineering, West Anhui University, Lu'an 237012, Anhui, People's Republic of China

³Research Center of Atoms Molecules and Optical Applications, West Anhui University, Lu'an 237012, Anhui, People's Republic of China

*Email address: tbhoang@memphis.edu

We report an optical study of the dynamics of photoexcited carriers in Si_2Te_3 nanowires at various temperatures and excitation powers. Si_2Te_3 nanowires were synthesized, by using gold as a catalyst, on a silicon substrate by the chemical vapor deposition method. The photoluminescence spectrum of Si_2Te_3 nanowires was primarily dominated by defect and surface states related emission at both low, and room temperatures. We observed that the decay time of photoexcited carriers was very long (> 10 ns) at low temperatures and became shorter (< 2 ns) at room temperature. Further, the carrier decay time became faster at high excitation rates. The acceleration of the photoexcited carrier decay rates indicates thermal quenching and structural modification along with the non-radiative recombination at high temperature and excitation power. Our results have quantitatively elucidated decay mechanisms that are important towards understanding and controlling the electronic states in Si_2Te_3 nanostructures for optoelectronic applications.

I. INTRODUCTION

Recent advances in semiconductor growth techniques have enabled the synthesis of a new class of silicon telluride (Si₂Te₃) nanostructures such as nanoplates,¹⁻³ nanobelts (nanoribbons)^{1,4} and nanowires (NWs).⁴ Si₂Te₃ exhibits interesting structural,^{2,5,6} optical,^{2,3,7,8} electrical,^{9,10} chemical^{1,3} and thermal^{11,12} properties which promise potential applications ranging from thermo-electrics to optoelectronics. Bulk Si₂Te₃ was reported to have an indirect electronic band structure.⁷ 2D Si₂Te₃ was also being investigated recently and it is interesting that the structural characteristics of this material might vary significantly depending on an array of parameters, therefore the resulting band

structure is also varying. For instance, the band gap can vary up to 40% along with a 5% change in the lattice constant depending on the orientations of the silicon dimers, which locate in between Te atoms.⁶ In any case, while the optical, electrical, and thermal properties of bulk Si₂Te₃ were explored several decades ago, these properties of nanostructured Si₂Te₃ have only been examined in the last several years. Indeed, there have been several papers reported on the optical properties of nanoplates¹⁻³ and nanobelts (nanoribbons),^{1,4} but so far none have reported any study on the dynamics of photoexcited carriers in Si₂Te₃ NWs, which is crucial information for any application in optoelectronics. One of the challenges in investigating physical properties of nanostructured Si₂Te₃ is the stability of the material under ambient conditions. This is due to the large surface to volume ratio at the nanoscale that leads to the surface reaction to the water vapor in the atmosphere, resulting a thin Te layer. Furthermore, the complication of the structural properties of Si₂Te₃ at low dimensions due to the orientation of the silicon dimers at different temperatures and strain could also lead to strikingly different optical or electronic properties.⁶ On the other hand, these dependencies also offer an opportunity such that properties of Si₂Te₃ nanostructures are controllable using this set of parameters. Further, while Si₂Te₃ material can be processed using standard semiconductor techniques, it is highly sensitive to environment which offers an advantage for chemical sensing applications.^{1,3}

In this work, we study the dynamics of photoexcited carriers in ensembles of Si₂Te₃ NWs as functions of temperature and excitation power. The Si₂Te₃ NWs were grown directly on silicon substrate, making them possible to integrate with other future optoelectronic devices.¹³⁻¹⁵ We observed that the photoluminescence (PL) intensity and decay time of photoexcited carriers vary significantly under different measurement conditions. Specifically, the emitted photons exhibited a long decay time (> 10.0 ns) at low temperature (< 100 K) but much shorter (~ 1.8 ns) at room

temperature, which is associated with an abrupt reduction in the intensity. Further, at any given temperature, the decay time reduced as a result of the increasing excitation power. These results indicate a significant non-radiative recombination rate associated with defects/surface states. Increased temperature could also change the crystal structure of the nanowires which led to modification of the band structure and the carrier dynamics. Our study offers an insight into the decay dynamics of photoexcited carrier and hints possible applications of the Si₂Te₃ nanowires in optoelectronics.

II. EXPERIMENTAL DETAILS

Tellurium (Te, 30 mesh, 99.997%, Aldrich) and silicon (Si, 325 mesh, 99%, Aldrich) powders were purchased from Sigma Aldrich and used as source materials for Si₂Te₃ nanowire growth. In order to initiate the nanowire growth, a layer of gold (Au) nanoparticles (5-10 nm in diameter) was spin coated onto Si or SiO₂ substrates. Both the Te and the Si powders were placed in a ceramic crucible and loaded into a high temperature quartz tube furnace while the substrates were placed downstream of the gas flow in the furnace. The quartz tube was first vacuum evacuated and then followed up by the introduction of high purity nitrogen gas (> 99.995%) with a mass flow rate of 15 sccm to maintain the starting pressure at 9.12 Torr. The furnace was heated from the room temperature at 20 °C/min and maintained at 850 °C for Si₂Te₃ nanowire growth for 5 min. After growth, the ceramic crucible and substrates were then cooled down to room temperature. Further, in order to minimize the surface reaction to the water vapor in the atmosphere, the freshly grown Si₂Te₃ nanowires were immediately transferred to a vacuum storage container or an optical cryostat for optical measurements.

In the experimental procedure ensembles of Si₂Te₃ nanowires were optically excited by an ultrafast laser (Coherent Chameleon Ultra II, 80 MHz, 150 fs). The output (950 nm) of the laser was

frequency doubled (to 475 nm) and focused onto the sample, via an 20X objective lens, with an excitation spot size $\sim 3~\mu m$. The average laser excitation power was $100~\mu W$ (measured before the objective lens); however, for the power dependent experiments the laser power varied. Si₂Te₃ nanowire sample was mounted onto the cold finger of a closed-cycle cryostat (Janis model CCS-XG-M/204N). The temperature of the cryostat can be controlled to allow optical measurements from 7-300~K. The PL signal was collected by the same objective lens, analyzed by a spectrometer (Horiba iHR550), and then detected by a CCD (Charged-Coupled Device) camera (Horiba Synapse). For the time-resolved single photon counting measurements, PL signal was filtered by a long pass filter and collected by a fast-timing avalanche photodiode (APD-PDM, Micro Photon Device). A time-correlated single photon counting module (PicoHarp 300), with a time bin of 4 ps, was used to analyze the number of photons as a function of time when they arrived at the photodiode. Final lifetimes were obtained from fits to the data de-convolved with the instrument response function. ¹⁶

III. RESULTS AND DISCUSSIONS

Si₂Te₃ NWs were first characterized by the scanning electron microscopic (SEM) method. Figure 1a shows a representative SEM image where as grown Si₂Te₃ NWs were randomly oriented on a silicon substrate. Individual nanowires have diameter and length vary around 300 nm and 10 μm, respectively. Even though most of NWs were straight and relatively uniform in diameter, it appeared that the NWs exhibited rough surfaces which could eventually affect the optical properties as we will discuss below. Further, due to the random orientation of the NW ensembles in the optical experiments, we have circularly polarized the laser excitation so that several NWs were somewhat equally excited in terms of polarization.

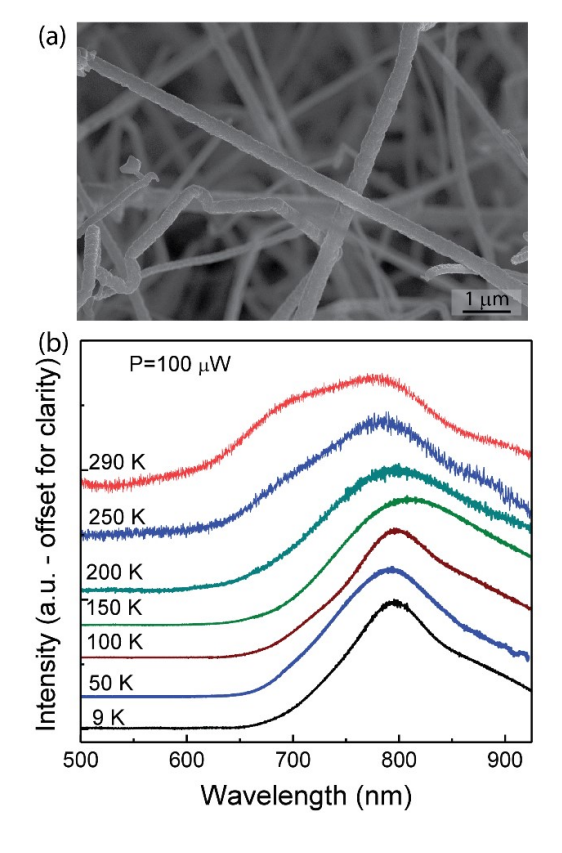


Figure 1. (a) SEM image of NW ensemble on a silicon substrate. (b) Normalized PL emission spectra of an NW ensemble at various temperatures (9 - 290 K). The spectra were vertically offset for clarity.

Figure 1b shows the normalized PL emission spectra of a NW ensemble at various temperatures (9-290 K) and at a fixed laser excitation power $P=100 \text{ }\mu\text{W}$. At low temperature (< 100 K) the PL spectrum featured by a broad peak at around 790 nm with a full-width-half-maximum (FWHM) $\sim 90 \text{ nm}$ and a shoulder at a longer wavelength ($\sim 890 \text{ nm}$). Similar results were observed earlier by Wu et al.² for Si₂Te₃ nanoplates where these two emission bands were assigned as defect emissions associated with thermal quenching as the temperature increased. However, it is noted that in this work we did not observe the band gap PL emission near 563 nm (2.2 eV for bulk Si₂Te₃).^{2,7,8,11} This could be due to different excitation conditions (pulsed vs continuous laser),¹⁷ crystal quality, or a modification of the band structure in these NWs which are caused by the reorientation of the Si dimers.⁶ Due to the recombination at trap states above the valence band¹¹

we can also note that some PL emission bands from bulk Si₂Te₃ were previously observed to exhibit at very low energies (~ 1.1 eV or > 1100 nm). These emission bands were not detected in our experiment due to a limitation of the silicon CCD, and other optics. At higher temperatures, another shoulder appeared at around 700 nm and became more dominant at 290 K. This additional shoulder likely originated from defect centers located at higher energy levels (within the band gap), and will only be populated at high temperatures or at high excitation powers. The PL emission at various temperatures is further analyzed in Fig. 2 which displays the temperature dependence of integrated PL intensity at temperatures from 9 K to 290 K. At low temperature (< 75 K) the total emitted intensity is high and fairly constant; however, above 75 K the intensity is abruptly reduced. This is similar to previously observed behavior of Si₂Te₃ nanoplates.² The inset in Fig. 2 displays the laser excitation power dependence of the total integrated PL intensity at temperature T = 9 K. It is clear that below a certain excitation value (< 250 μW) the PL intensity increased linearly with the increasing excitation power. Above 250 µW, a saturation behavior occurred which was a result of the reduction in the absorption efficiency. It was also possible that at high excitation powers, the high average number of photoexcited carriers led to the non-radiative recombination with the surface states and resulted in nonlinear relaxation processes (i.e. Auger recombination) which are characterized by a reduction in the photon decay time.

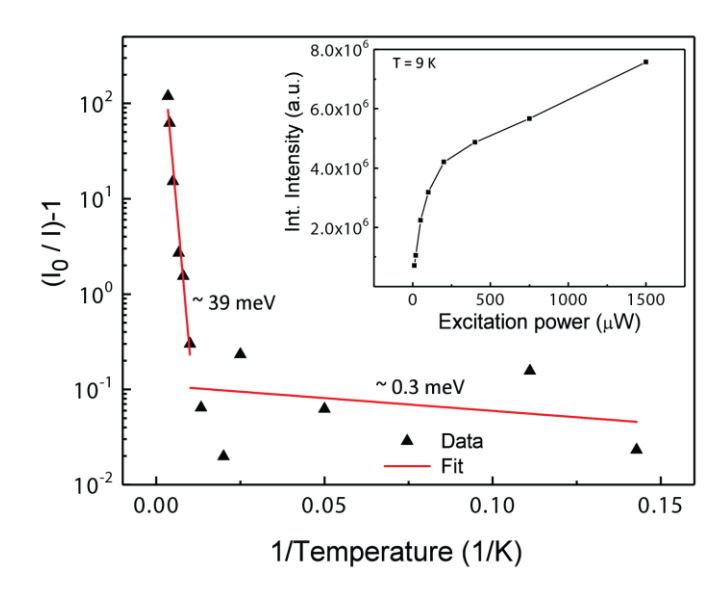


Figure 2. Temperature dependent integrated PL intensity at a fixed average excitation power $P = 100 \mu W$. I and I_0 are the PL intensities at a given temperatures T and at 0K, respectively. Red lines are fits to the data. Inset: Excitation power dependent PL emission intensity at temperature T = 9 K.

In the previous study by Wu et al,² by measuring the PL spectra at different temperatures of Si2Te3 nanoplates the authors have extracted very large activation energies which indicated that several thermal related processes have occurred. Here we also observed a large activation energy of E = 39 meV at temperature above 75 K. The red lines in Figures 2 were the fits according to $I_0/I - 1 = exp(-E/k_BT)$ where I and I₀ are the PL intensities at temperatures T and at 0K, respectively. This activation energy is even larger than the value of the thermal energy k_BT at room temperature (~25.7 meV) which suggests that the energy transition of the photoexcited carriers was not purely promoted by the thermal energy but rather a thermal-induced modification of the defect related state energy levels. For instance, defects related to impurities, rough surfaces (Fig. 1(a)), or structural/chemical modifications could transform to metastable configurations with different energy levels under thermal and optical excitations. A well-known case is the DX center in III-V semiconductors. Such metastable configurations can affect the decay of photoexcited carriers differently, and their populations depend on temperature and excitation rate. This hypothesis is

further supported by the decay dynamic measurements of the photoexcited carrier as we will present in sections below.

In order to gain further insight into the dynamics of the photoexcited carriers we performed the temperature dependent time-resolved measurements (Figure 3). At low temperatures (< 100 K) and low excitation power ($< 100 \mu W$) the decay time of the photoexcited carriers was characterized by a straight line, indicating a long decay time of the excitonic states. Indeed, given 80 MHz of the laser used for this study, we could not perform a fitting procedure to deduct the long decay times for these measurement conditions. This result is consistent with a previous study which concluded a long hole's lifetime in bulk Si₂Te₃. 11 At around 150 K, a decay trace could be observed with a single decay component that has a decay time ~ 10 ns at 100 μ W excitation power. At higher temperatures, the decay time became faster and at 290 K it was determined to be 1.83 ns. A significant reduction of the decay time when the temperature increased indicated several effects. First, there was a thermalization process of neutral donors and thermal quenching of the photoexcited carriers. This is consistent with the observation that there was a significant reduction in the total integrated PL emission intensity (Fig. 2). The thermal processes led to an increase in the non-radiative recombination rate and eventually a reduction in the decay time of the emitted photons. Secondly, following the work by Shen et al. there could be a re-arrangement in the structural configuration of the Si₂Te₃ lattice at different temperatures which resulted in a modification in the band structure and carrier dynamics.⁶

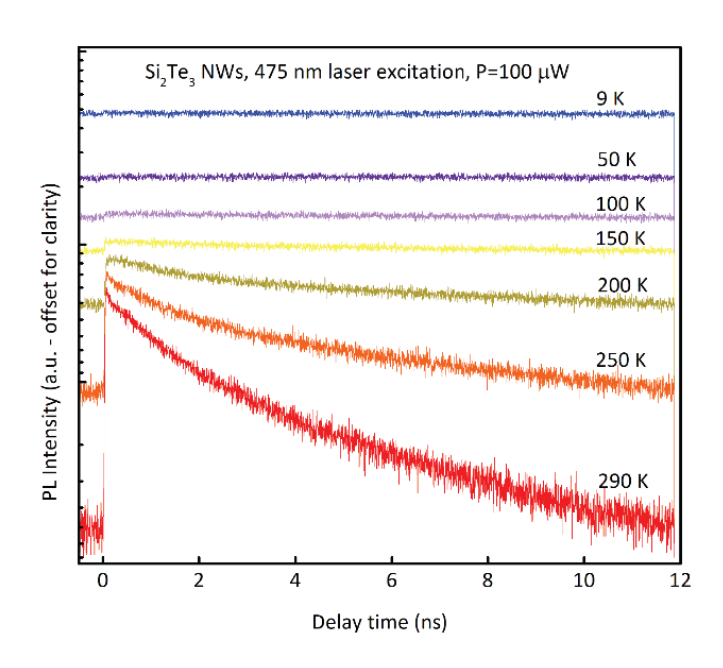


Figure 3. Measured decay curves at different temperatures at a fixed average excitation power $P = 100 \mu W$.

The decay dynamics of the photoexcited carriers in Si_2Te_3 nanowires could also be associated with the carrier generation rate, which is directly related to the incident laser excitation power. Figure 4 shows the decay dynamics of Si_2Te_3 NW ensembles in a matrix of parameters. Specifically, we have measured the decay times of these NWs at various incident laser excitation powers and temperatures. At low excitation powers (< 100 μ W) and low temperatures (< 100 K), the decay curves featured by flat lines from which the decay time could not be determined at least from our current apparatus. At below 100 K, by increasing the excitation power (to above 150 μ W), a single exponential decay component could be observed. For instance, at 9 K the decay time was determined to decrease from 7.25 ns to 6.08 ns when the excitation power increase from 200 to 750 μ W (Fig. 4(a)). Other similar measurements at temperatures 50-290 K are shown in Figs. 4(b)-(f). At room temperature (290 K), the decay time reduced from 1.88 ns to 1.73 ns as the excitation power increased from 20 – 750 μ W. The temperature and power excitation dependences imply that, even at low temperature, the high excitation rate has led to a non-radiative recombination of

the photoexcited carriers (due to surface states, for instance). At higher temperature (> 150 K), the decay time became faster even at low excitation rates, which was the result of thermal effect.

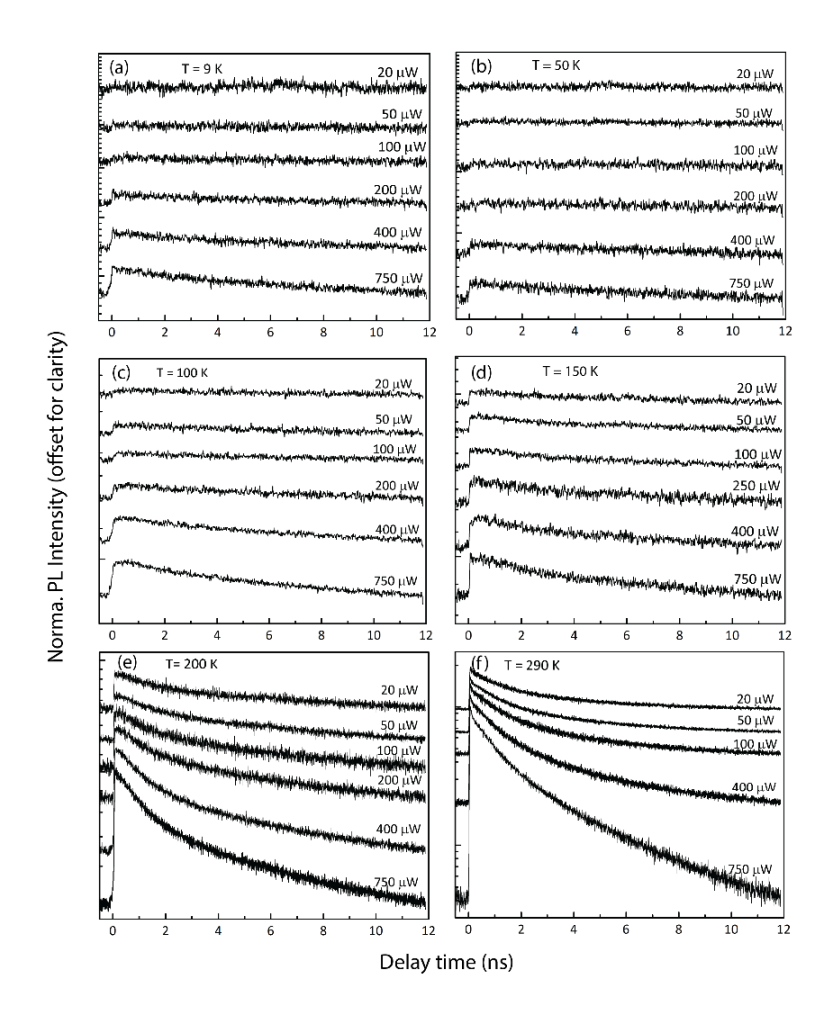


Figure 4. Excitation power dependent decay dynamics at different temperatures (a-f) \rightarrow (9-290 K). At each temperature, the excitation power was varied from 20 μ W to 750 μ W.

At high temperatures (> 150 K) the decay times from Si₂Te₃ NWs decreased with increasing excitation power and indeed exhibited bi-exponential decay behavior. Besides the fast decay component (for instance, decay time ~1.73 ns at 750 μW, Fig. 4(f)), there was also a slower component which varied from 3.05 to 2.40 ns depending on the excitation power and temperature. The bi-exponential decay behavior of the photoexcited carriers in Si₂Te₃ NWs was associated with a spectral modification under various excitation powers. Fig. 5 shows the emission spectra for

different excitation powers at T = 290 K which clearly indicates that at high excitation powers there was an additional shoulder peak at around 680 nm. It is likely that this additional energy transition peak, which associated with defect centers, surface states or band structure modification, has contributed to the bi-exponential decay components of the decay curves shown in Figs. 4 (e-f). A spectrally resolved decay time measurement in the future could potentially help to relate the emission energies with the fast and slow decay components.

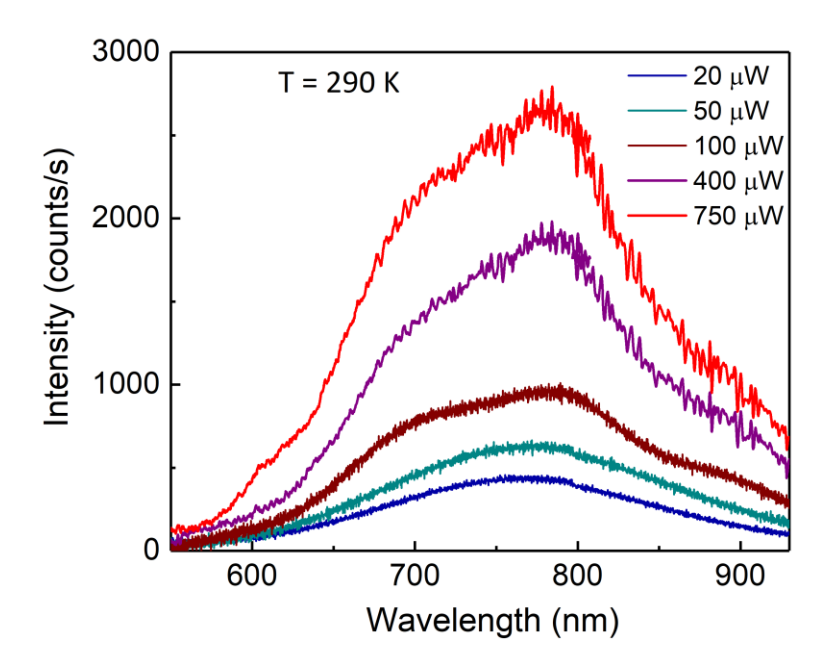


Figure 5. Excitation power dependent PL emission spectra at T = 290 K.

One another possible mechanism which could lead to the shorter decay time at higher temperature and excitation rate is due to the modification of the band structure as the result of changes in the orientation of the Si dimers with respect to the Te atoms.⁶ This could be further complicated by the fact that there were boundaries between different crystal domains, which may have different orientation of the dimers. The energy offsets between domains, depending on the temperature, could result in an indirect transition and therefore a different decay time. The current available data achieved in this study did not allow us to draw a direct conclusion regarding a specific band

alignment but rather hinted several mechanisms for the decay dynamics of the photoexcited carriers. Nevertheless, we would like to point out that several previous experimental studies^{5,19} on bulk Si₂Te₃ have indicated that different domains of the Si dimers' orientation do exist. Density functional theory calculation has also suggested that different domains exist with different orientations of the Si dimers.⁶ Future measurements such as polarized decay dynamics from single Si₂Te₃ NWs in different excitation conditions, and in combination with structural characterizations (SEM or TEM – Transmission Electron Microscopy) to correlate structural characteristics with optical properties of the same single NWs could potentially provide further information. Finally, we would like to note that even though the Si₂Te₃ NWs used for this study were grown at high temperature (~850 oC) and used Au nanoparticles as catalysts, other Si₂Te₃ nanostructures such as Si₂Te₃ nanoplates^{2,4} can be grown at lower temperature (~600 oC) and without use of Au catalysts and have a potential for CMOS-compatible devices. Stacking of many nanoplates in the vertical direction could also lead to Si₂Te₃ NW formation.

VI. CONCLUSIONS

In conclusion, we have investigated the decay dynamics of the photoexcited carriers in ensembles of Si₂Te₃ NWs as functions of temperature and excitation rate. We have observed a combination of carrier thermalization and possible band structure modification. Our results have revealed the decay dynamics of Si₂Te₃ NWs in a matrix of parameters which could be used to control the physical characteristic of the materials for possible applications in optoelectronics and thermoelectric.

ACKNOWLEDGMENTS

This work was supported by the National Science Foundation (NSF) (DMR-1709528 and DMR-1709612), by the Ralph E. Powe Junior Faculty Enhancement Award from Oak Ridge Associated

Universities (to XS), and in part by a grant from The University of Memphis College of Arts and Sciences Research Grant Fund (to TBH). This support does not necessarily imply endorsement by the University of research conclusions.

REFERENCES

- Sean Keuleyan, Mengjing Wang, Frank R. Chung, Jeffrey Commons, and Kristie J. Koski, Nano Letters **15** (4), 2285 (2015).
- Keyue Wu, Weiwei Sun, Yan Jiang, Jiyang Chen, Li Li, Chunbin Cao, Shiwei Shi, Xiao Shen, and Jingbiao Cui, Journal of Applied Physics **122** (7), 075701 (2017).
- Mengjing Wang, Gabriella Lahti, David Williams, and Kristie J. Koski, ACS Nano **12** (6), 6163 (2018).
- Keyue Wu and Jingbiao Cui, Journal of Materials Science: Materials in Electronics **29** (18), 15643 (2018).
- K. Ploog, W. Stetter, A. Nowitzki, and E. Schönherr, Materials Research Bulletin 11 (9), 1147 (1976).
- X. Shen, Y. S. Puzyrev, C. Combs, and S. T. Pantelides, Applied Physics Letters **109** (11), 113104 (2016).
- A. P. Lambros and N. A. Economou, physica status solidi (b) 57 (2), 793 (1973).
- U. Zwick and K. H. Rieder, Zeitschrift für Physik B Condensed Matter **25** (4), 319 (1976).
- ⁹ H. P. Bauer and U. Birkholz, physica status solidi (a) **49** (1), 127 (1978).
- M. Rick, J. Rosenzweig, and U. Birkholz, physica status solidi (a) **83** (2), K183 (1984).
- 11 K. Ziegler and U. Birkholz, physica status solidi (a) **39** (2), 467 (1977).
- Rinkle Juneja, Tribhuwan Pandey, and Abhishek K. Singh, Chemistry of Materials **29** (8), 3723 (2017).
- Saniya Deshpande, Indrasen Bhattacharya, Gilliard Malheiros-Silveira, Kar Wei Ng, Fabian Schuster, Willi Mantei, Kevin Cook, and Connie Chang-Hasnain, ACS Photonics 4 (3), 695 (2017).
- Fanglu Lu, Indrasen Bhattacharya, Hao Sun, Thai-Truong D. Tran, Kar Wei Ng, Gilliard N. Malheiros-Silveira, and Connie Chang-Hasnain, Optica 4 (7), 717 (2017).
- Jesper Wallentin, Nicklas Anttu, Damir Asoli, Maria Huffman, İngvar Åberg, Martin H. Magnusson, Gerald Siefer, Peter Fuss-Kailuweit, Frank Dimroth, Bernd Witzigmann, H. Q. Xu, Lars Samuelson, Knut Deppert, and Magnus T. Borgström, Science 339 (6123), 1057 (2013).
- Jörg Enderlein and Rainer Erdmann, Optics Communications **134** (1), 371 (1997).
- Jiani Huang, Thang B. Hoang, and Maiken H. Mikkelsen, Scientific Reports **6**, 22414 (2016).
- P. M. Mooney, in *Deep Centers in Semiconductors: A State-of-the-Art Approach*, edited by Sokrates T. Pantelides (CRC Press, 1992), pp. 643.
- P. E. Gregoriades, G. L. Bleris, and J. Stoemenos, Acta Crystallographica Section B **39** (4), 421 (1983).